Supporting Information

Conjugation Efficiency of the Laser Based Bioconjugation of Gold Nanoparticles with Nucleic Acids

Svea Petersen, Stephan Barcikowski*

Laser Zentrum Hannover e.V.
Hollerithallee 8
30173 Hannover
Germany
Tel +49 511 2788377
Fax +49 511 2788100
e-mail: s.barcikowski@lzh.de

Nanoparticle Characterization

Transmission electron microscopy was used to determine the size distribution of resulting nanoparticles. Samples for TEM analysis were prepared by placing a drop of nanoparticle dispersion, as obtained by laser ablation, on a carbon coated, formvar-covered copper grid, and dried at room temperature. At least 500 nanoparticles were sized from TEM micrographs, which revealed three significantly different size distributions in dependance of the ssO concentration (Fig S1).

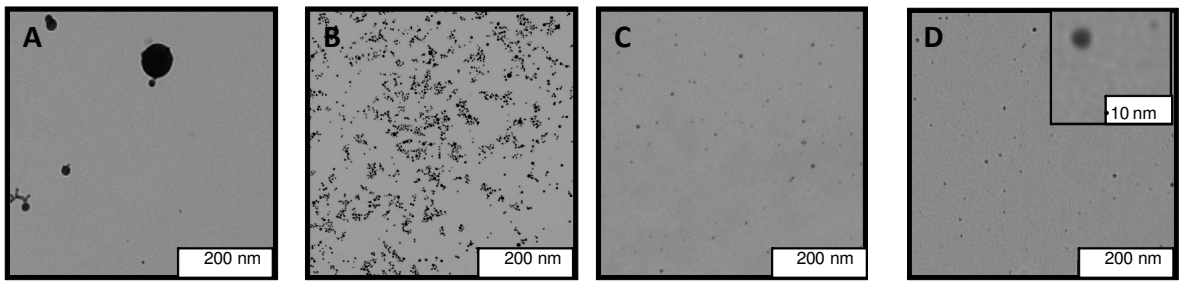

Figure S1. TEM analysis of nanoparticles generated in increasing thiolated oligonucleotide (HS-ssO) concentrations (A: no ssO, B: 0.1 µM ssO, C: 0.5 µM ssO, D: 5 µM ssO).

One observes a size quenching with increasing HS-ssO concentrations, which reaches its maximum at 0.5 µM (Fig S2). The average diameter of a typical particle preparation at HS-ssO concentrations higher than or equal to 0.5 µM is 5.0 ± 1.3 nm. An HS-ssO concentration of 0.1 µM and 0.25 µM results in slightly bigger nanoparticles with an average diameter of 5.7 ± 3.4 nm. No significant difference was observed in the size of nanoparticles generated in 0.1 and 0.25 µM. Generation of gold nanoparticles in water leads to the typical broad distribution with an average Feret diameter of 15.0 ± 10.3 nm (Fig S1 A), as there is no competition between growth and surface coating.

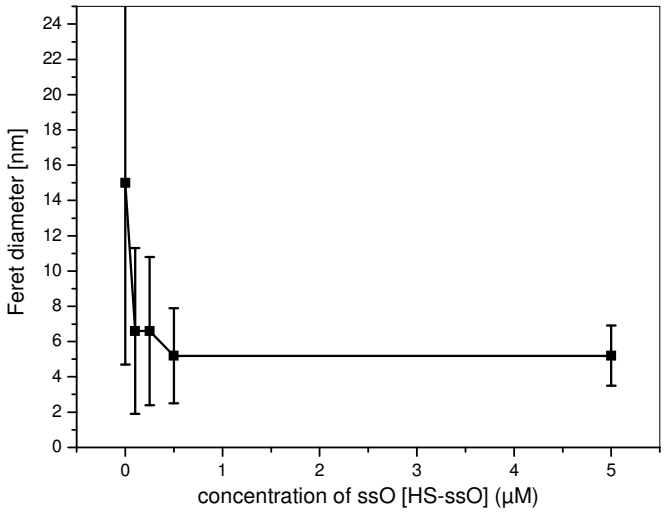

Fig S2. Average Feret diameter of laser generated gold nanoparticles as function of the added oligonucleotide concentration.

Number, mass and surface weighted size distributions of the three different kinds of nanoparticles are displayed in Figure S3. While the mass weighted size distribution is applied for the calculation of molar nanoparticle concentrations, the surface weighted distribution is used for the determination of surface coverages.

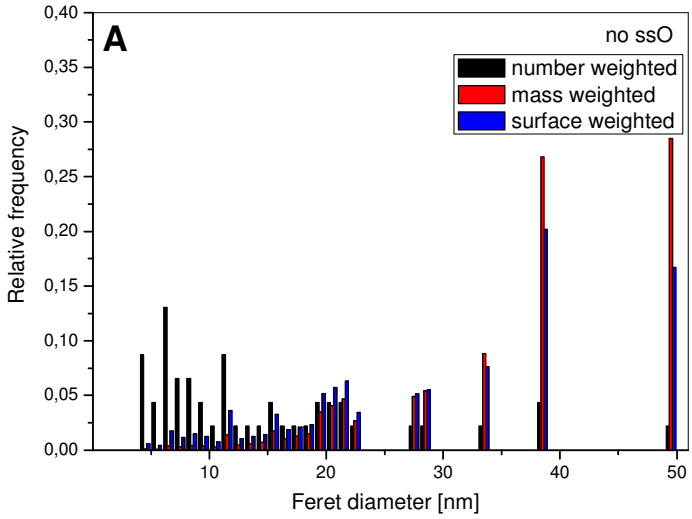

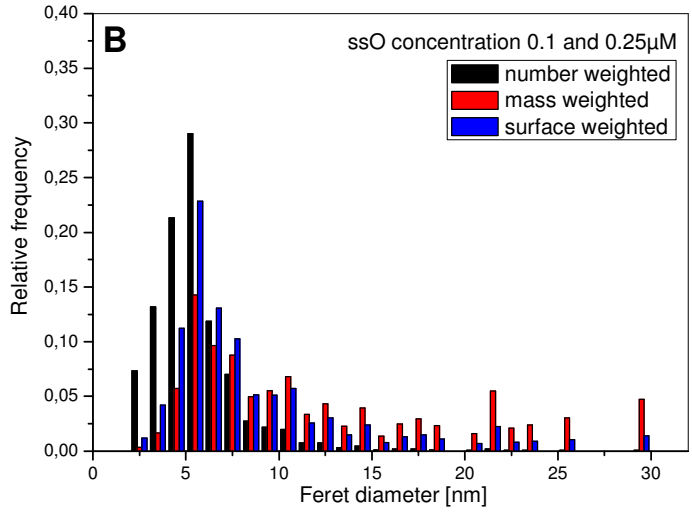

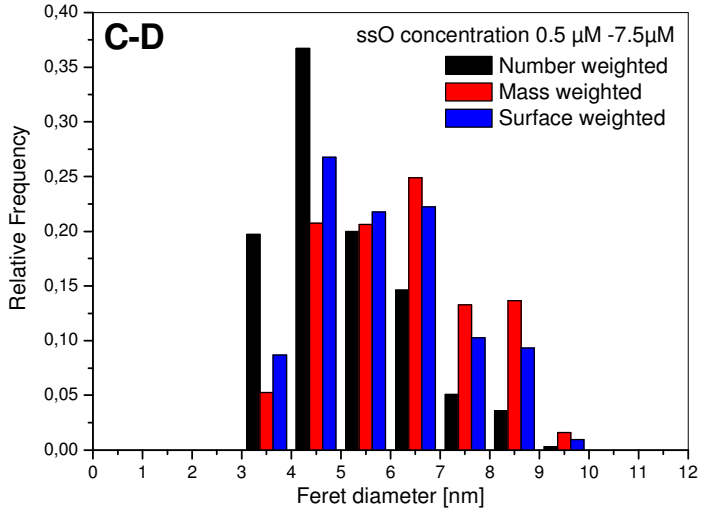

Fig S3. Number, mass and surface weighted size distributions of nanoparticles generated in increasing oligonucleotide concentrations (A: no ssO, B: 0.1 µM; 0.25 µM ssO, C: 0.5 µM ssO; D: 5 µM ssO).

Calculated average particle masses and surface areas are shown in Table S1.

Table S1. Average particle mass and average particle surface area

	Average particle mass [g]	Average particle surface [cm^2]
in situ conjugation (ssO ≥ 0.5µM)	1.54E-18	8.36E-13
in situ conjugation (ssO < 0.5 µM)	3.47E-18	12.17E-13
Ex situ conjugation	94.50E-18	101.34E-13

UV Vis spectroscopy, performed with a Shimadzu 1650 confirms the broader size distribution of gold nanoparticles generated in water compared to bioconjugates.

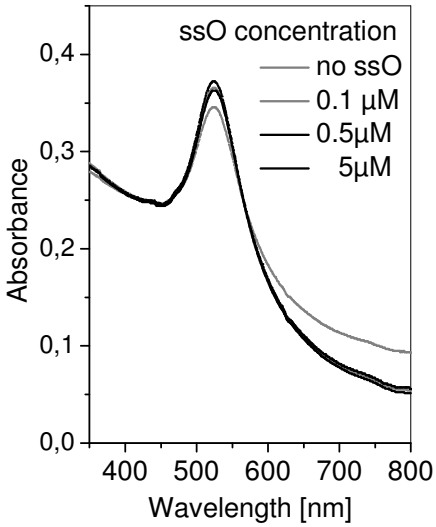

Fig S4. UV Vis spectroscopy of gold nanoparticles generated by laser ablation in different ssO concentrations.

Nanoparticle mass was controlled via weighing the target before and after each ablation process. The resolution of the balance reaches down to 1 µg, which results in a measurement error in nanoparticle concentration of 4 µg mL^{-1}, as we deal with mass differences. Since this fact has an equal impact on each of the three determination methods, error bars were exclusively added for the indirect determination of the surface coverage by remaining HS-ssO in the supernatant after in situ conjugation in Figure 2.

Quantification of ssO loaded on gold nanoparticles

Excess oligonucleotides were removed by centrifugation of nanoparticle suspensions for 30 min at 40,000 g. The resulting supernatant was stored for further analysis. In the case of HS–ssO-Alexa 488 conjugation, the red precipitate was then washed twice with ddH_2O by successive centrifugation and redispersion and then finally taken up in 200 µL of an aqueous solution of 5 mM dithiothreitol (DTT). After 18 h at room temperature with intermitting shaking, the solutions containing the displaced HS–ssO-Alexa 488 were separated from the gold by a second centrifugation. Absorbance corresponding to excess ssO (260 nm) in the first

supernatant (see Fig S6) and absorbance at 496 nm corresponding to displaced Alexa 488 labeled ssO (see Fig S7) in the second supernatant was recorded with a Shimadzu 1650 UV-VIS spectrometer. Intensities were converted to molar concentrations of HS-ssO-X by interpolation from a linear standard calibration curve. Standard curves were prepared with known concentrations of HS-ssO-X (see Fig S5). Finally, the average number of HS-ssO-X per particle was obtained by dividing the measured HS-ssO-X molar concentration by the original nanoparticle concentration. Normalized surface coverage values were then calculated by dividing the estimated particle surface area (assuming spherical particles) in the nanoparticle suspension.

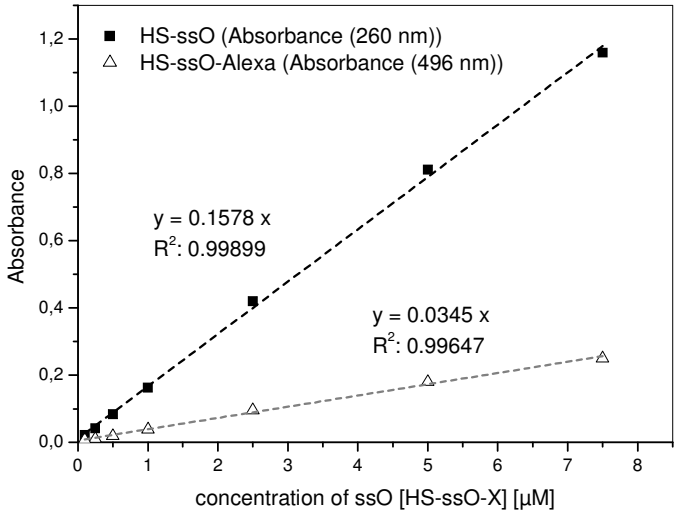

Figure S5. Standard calibration line of the unlabeled oligonucleotide (HS-ssO) and the Alexa labeled oligonucleotide (HS-ssO-Alexa) at 260 and 496 nm respectively

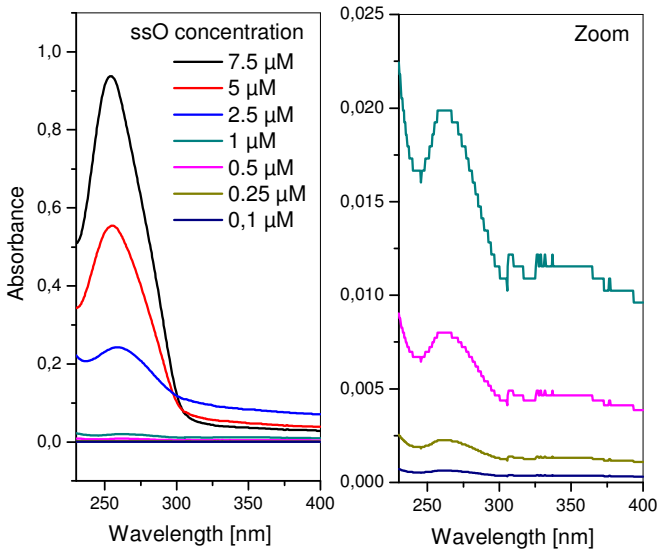

Fig S6. UV spectra of remaining unlabeled ssO in the supernatant 1 after in situ conjugation at various HS-ssO concentrations

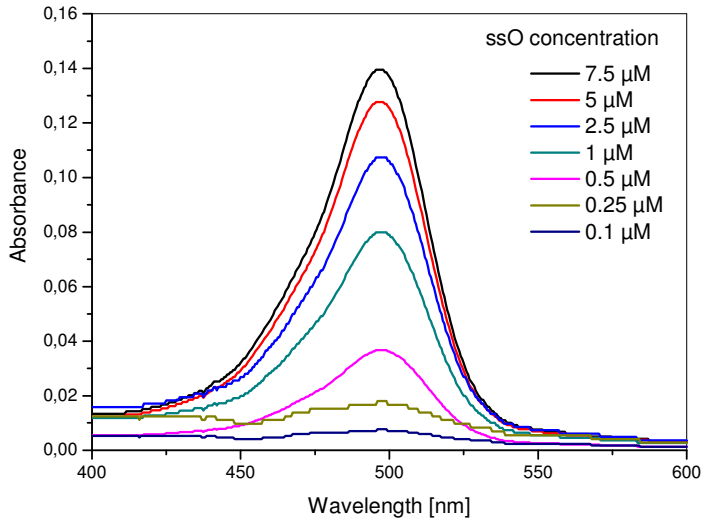

Fig S7. Vis spectra of conjugated HS-ssO-Alexa in the supernatant 2 after ligand exchange with dithiothreitol and previous in situ conjugation at various HS-ssO-Alexa concentrations.

Quantification of recoverage or degradation of ssO after ligand exchange

25 µL of a 100 mM aqueous DTT solution were added to 475 µL colloid after conjugation with ssO. Following centrifugation after 18 h of co-incubation, absorbance at 496 and 648 nm was measured to estimate the concentration of displaced Alexa 488 and Cy 5 respectively. Values after ex situ conjugation correspond to the recoverage after DTT displacement and after in situ conjugation to the sum of recoverage after DTT displacement and degradation due to laser irradiation.

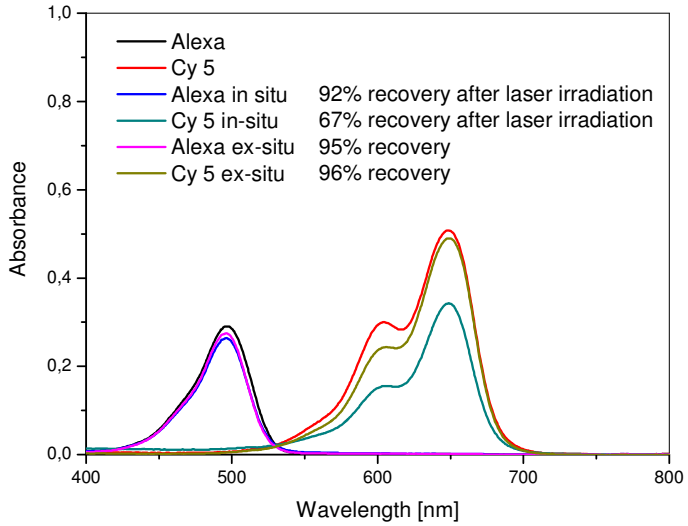

Fig S8. Vis spectra of Alexa 488 and Cy5 labeled oligonucleotides before the conjugation process, after ex-situ conjugation and in-situ conjugation with 5 µM HS-ssO-X.

While recoverage of the fluorophores was checked by Vis spectroscopy (Fig S8), the analysis of oligonucleotides was performed by polyacrylamide gel electrophoresis. Quantification of DNA with its characteric absorbance band at 260 nm was not possible due to a coabsorbance of the ligand exchange agent dithiothreitol.

For 20% gels, 20 mL of an acrylamide/bis-acrylamide (37.5:1) solution was mixed with 14.4 g urea and 2.5 mL 10xTBE buffer. The mixture was heated above 37°C to dissolve the urea. 7.5 ml water, 150 µL 10 % ammonium persulfate and 75 µL tetramethylethylendiamin

were added. The mixture was swirled and then immediately poured in a gel tray (Maxi (20x20 cm) CTV400, VWR) and let to polymerize for 2 hours. To denature the oligonucleotides, 10 µL of formamide was added to 50 µL of each supernatant and the mixture was heated 2 min at 95°C. 20 µL of a loading buffer containing 75 % glycerol, 0.125 % bromphenol blue and 0.125 % xylene cyanole was added. The references, containing the initial concentration of oligonucleotide, omitted the laser irradiation and were treated equally before gel electrophoresis and run with the samples on each gel. 10 µl of sample was loaded in each well. Gels were run 3 hours at 300 V in 1 x TBE buffer (pH around 8.3 - 8.5). To visualize the bands on the gel after gel electrophoresis, gels were fixed in 30 % EtOH, 10 % glacial acid for 30 min. After thoroughly rinsing, the gels were stained and developed using Fast*Silver*^{TM} (G Biosciences, USA). Scans of resulting stained gels were analysed with Image J. The intensity of the bands (I(x)) was compared to the references (I(0)) in order to deduce the degree of recovered oligonucleotide after conjugation and/or laser ablation by equation 3.

$$Deg\ (x) = 1 - I(x)/ I(0) \qquad (3)$$

Further additional figures and tables

While the size quenching during in situ conjugation has been already discussed, after ex situ conjugation no difference was observed in the Feret diameter distribution of the gold nanoparticles. A look at the hydrodynamic size distribution revealed a slight increase of 2 nm due to the increased solvatisation shell of charged HS-ssO (Fig S9). The hydrodynamic size was determined by Dynamic Light Scattering with the Zetasizer ZS (Malvern). Three consecutive measurements are carried out and mean values are presented.

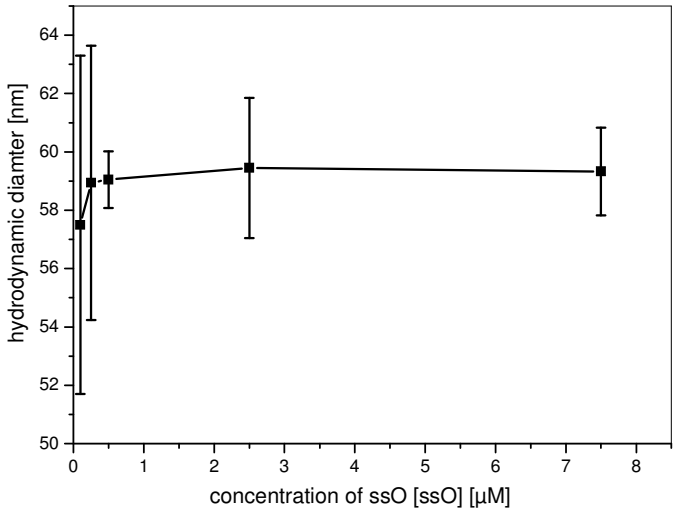

Fig S9. Average hydrodynamic diameter of ex-situ conjugated gold nanoparticles with increasing ssO concentrations.

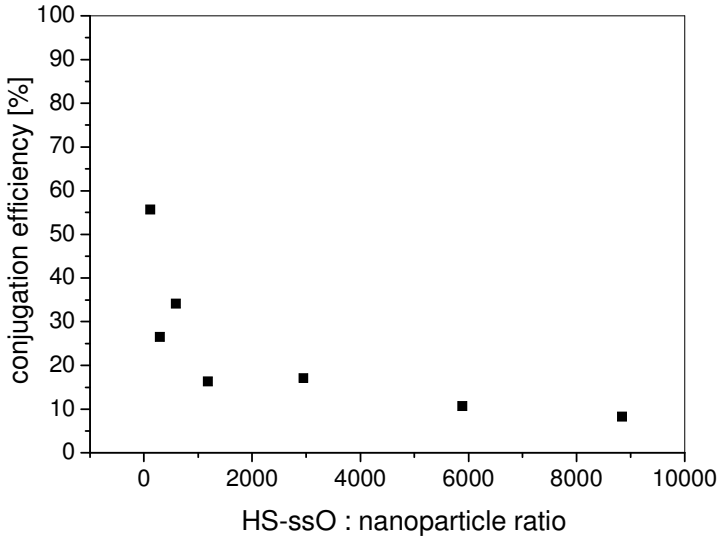

Figure S10. Conjugation Efficiency of the ex situ conjugation

Table S2. Surface coverage values for chemically synthesized gold nanoparticles conjugated by ligand exchange reactions reported in literature.

Base length	Anchoring group	surface coverage [pmol cm^{-2}]	Ref
12	3' R-S-S-R	7.5	26
22	3' R-S-S-R	12.0	26
22	3' R-S-S-R	21.0	26
12	3'HS-R	12.6	26
22	3'HS-R	21.1	26
22	3'HS-R	12.2	26
12	5' HS-R	34	22
32	5' HS-R	15	22
32	3' HS-R	24	22
32	3' HS-R	35	22
23	5‘ HS-R	146	this paper